

# IN-SITU OBSERVATION OF S' PHASE IN Al-Li BASE ALLOY USING TEM SERIAL ROTATION TECHNIQUE<sup>①</sup>

Zhen, Liang Cui, Yuexian Sun, Dongli Yang, Dezhuang

*Harbin Institute of Technology, Harbin 150006, China*

## ABSTRACT

An in situ observation of the s' phase morphology and its orientation with the matrix in an Al-Li base alloy was carried out by means of double-tilt rotating around  $[220]_s$  in a transmission electron microscope (TEM). The results show that the s' phase precipitates in the form of bundles. The units of s' phase are lath-shaped, grow along the  $\langle 100 \rangle_s$  orientation, and have habit planes of  $\{210\}_s$ . Many units of the s' phase grow in the same orientation and get together to form a plate-shaped bundle of s' phase laths which lie on the  $\{110\}_s$  planes.

**Key words:** Al-Li base alloy s' phase in-situ observation TEM

## 1 INTRODUCTION

The s' phase is the most important precipitate in Al-Cu-Mg alloys. Previous papers<sup>[1-3]</sup> show that the s' phase precipitates in the form of lath, grows along the  $\langle 100 \rangle_s$  orientation and has the habit planes of  $\{210\}_s$ . In Al-Li-Cu-Mg alloys, the s' phase is also one of the most important strengthening phases, and can disperse planar slip and therefore, improve strength and ductility of the alloys<sup>[4-5]</sup>. Adding Cu and Mg to Al-Li base alloys so as to promote the precipitation of s' phase is the main purpose of alloying. However, the morphology and distribution of s' phase in Al-Li base alloys have not been completely understood up to date. In this paper, an in-situ observation of the s' phase in an Al-Li-Cu-Mg-Zr alloy has been carried out, using TEM serial rotation technique. The results

are of great importance both in theory and in practice for the understanding of the spacial morphology, habit planes and other crystallographic features of the s' phase.

## 2 EXPERIMENTAL PROCEDURE

The composition (wt.-%) of the alloy is: 1.94Li, 2.36Cu, 0.84Mg, 0.073Zr, balance Al. It was prepared by melting and casting under argon, and was homogenized at 510 °C for more than 24 h. After hot and cold rolling, the plate of 2 mm in thickness was obtained which was used to prepare specimens. The specimens were solution treated at 530 °C in KNO<sub>3</sub> salt bath for 30 min, quenched in cold water, and then artificially aged at 170 °C and 190 °C respectively. Microstructures were observed in a CM12/STEM transmission electron microscope at 120 keV. Foils were prepared with the standard twin-jet electropolishing technique.

<sup>①</sup>Manuscript received Jan.20, 1992

The electrolyte was a 30% nitric acid in methanol solution cooled to  $-20^{\circ}\text{C}$  with a potential of 15 V.

### 3 RESULTS

Observation results by TEM show that the  $s'$  phase precipitates in the form of plate-shaped bundles which are formed by lath-shaped  $s'$  phase units. Aging conditions have a little effect on volume fraction and morphology of the  $s'$  phase. In the specimens aged at  $170^{\circ}\text{C}$ , the plate-shaped bundles of  $s'$  phase laths have regular appearance and the laths in the bundles are thinner, as shown in Fig.1(a) and (b). But in the specimens aged at  $190^{\circ}\text{C}$ , the volume fraction of  $s'$  phase is less, and the gathering of  $s'$  phase laths is not evident. But when a 2% prior stretch is applied,

the volume fraction of  $s'$  phase in specimens aged at  $190^{\circ}\text{C}$  is greatly increased, and the  $s'$  phase get together again to form plate-shaped bundles. But the plate is less regular in shape, in which the laths are coarser and close to rod-shaped, as shown in Fig.1 (c) and (d).

In order to study the special morphology of the  $s'$  phase and its orientation relationship with the matrix, an in-situ observation of the  $s'$  phase in the specimen aged at  $170^{\circ}\text{C}$  for 140 h has been carried out by means of TEM serial rotation technique. The results are shown in Fig.2.

Fig.2 (b) is the  $[011]_s$  diffraction pattern. There are two kinds of typical morphologies in Fig.2. The precipitate A is thinner and longer, and the precipitates B and C are plate-shaped. On the basis of the  $[011]_s$  diffraction pattern, it

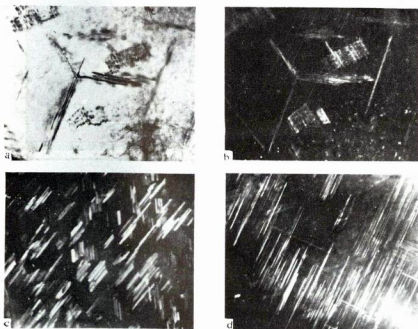


Fig.1 TEM micrographs showing morphology of  $s'$  phase in Al-1.94 Li-2.36 Cu-0.8 Mg-0.073 Zr alloy under various aging conditions

- (a)— $170^{\circ}\text{C} / 140\text{ h}$  bright field; (b)— $170^{\circ}\text{C} / 140\text{ h}$ , dark field; (c)—2% cold stretched  
+ $190^{\circ}\text{C} / 30\text{ h}$ , dark field; (d)—2% cold stretched + $190^{\circ}\text{C} / 100\text{ h}$ , dark field

can be determined that the orientation of long axis of the precipitate A is  $[100]_s$  and the stripes in the precipitates B and C have the orientation of  $[011]_s$ . After rotating  $35(^\circ)$  from the  $[011]_s$  zone axis, the bright field image of  $(111)_s$  foil plane and the  $[111]_s$  diffraction pattern were obtained, as shown in Fig.2 (c) and (d). In Fig.2 (c), it can be seen that the

shape of precipitate A has no change, while the plate-shaped precipitates B and C have changed.

Fig.2 (a) is the bright field image of  $(011)_s$  foil plane, and into the same as that of the precipitate A after rotating from  $[011]_s$  to  $[111]_s$  zone axis. From the  $[011]_s$  diffraction pattern, we can know the long axis of the precipitate A

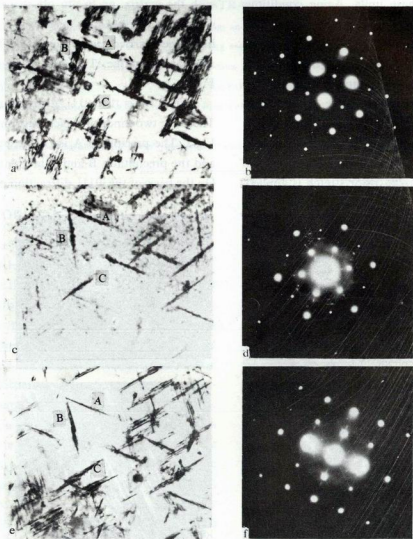


Fig.2 TEM micrographs obtained by serial rotation technique, showing morphologies of  $s'$  phase and corresponding diffraction pattern in various zone axes of the matrix

- (a)— Bright field image of  $(011)_s$  foil plane; (b)—  $[011]_s$  diffraction pattern; (c)— Bright field image of  $(111)_s$  foil plane; (d)—  $[111]_s$  diffraction pattern; (e)— Bright field image of  $(211)_s$  foil plane; (f)—  $[211]_s$  diffraction pattern

is  $[211]_x$  orientation, and that of the precipitates B and C are  $[112]_x$  and  $[121]_x$  respectively. Besides the bundles of *s'* phase laths which have a strong contrast, there are many stripes with very weak contrast to the matrix. The stripes are parallel to the bundle. When rotating  $20^\circ$  from  $[111]_x$  to  $[211]_x$  zone axis, the obtained bright field image of  $(211)_x$  foil plane and  $[211]_x$  diffraction pattern are seen in Fig.2 (e) and (f). And Fig.2 (e) shows that the morphology of precipitate A has no obvious change yet, and only its length has shortened a little. However, the precipitates B and C have widened, and many stripes parallel to each other can be seen among them. The precipitate A in Fig.2 (e) has long axis of  $[\bar{1}11]_x$  orientation, and the stripes in precipitates B and C have orientations of  $[2\bar{3}1]_x$  and  $[2\bar{1}5]_x$  respectively.

#### 4 DISCUSSION

Previous experimental investigations<sup>[1-3]</sup> have shown that the *s'* phase in Al-Cu-Mg alloys is lath-shaped, grows along the  $\langle 100 \rangle_x$  orientation and has the habit planes of  $\{210\}_x$ . Thus, it might be assumed that the plate-shaped bundles of *s'* phase are also lying on  $\{210\}_x$  planes. But such a suggestion can not explain the above results of observation. If the plate-shaped bundles of *s'* phase laths precipitate on  $\{210\}_x$  planes, then the precipitate A should lie on  $(0\bar{1}2)_x$  plane or  $(0\bar{2}1)_x$  plane, and the precipitates B and C on  $(102)_x$  plane and  $(\bar{1}20)_x$  plane respectively, as determined from their orientation with the matrix in Fig.2 (e). But the angle of  $(0\bar{1}2)_x$  or  $(0\bar{2}1)_x$  plane with the  $(211)_x$  foil plane is  $79.48^\circ$  and  $(\bar{1}20)_x$  or  $(102)_x$  planes are perpendicular to the  $(211)_x$  plane. As shown in Fig.2 (e), the width of the precipitate B or C is evidently larger than that of the

precipitate A, implying that the width of the image obtained from the plate-shaped bundle which is perpendicular to the foil plane is larger than that of the image obtained from the plate that has an angle of less than  $90^\circ$  with the foil plane. This is obviously not in accord with the fact of the matter. Also, if the *s'* phase lies on  $\{210\}_x$  planes, the fact that there exist strings along  $\langle 110 \rangle_x$  orientations in the diffraction patterns in Fig.2 can not be explained. These strings demonstrate that the plate shaped bundles of *s'* phase laths may lie on  $\{110\}_x$  planes, as shown in Fig.3. It can be seen that the units of *s'* phase are lath-shaped, grow along the  $\langle 100 \rangle_x$  orientation, and have the habit planes of  $\{210\}_x$ . Also many units of the *s'* phase get together, forming a plate-shaped bundle which lies on the  $\{110\}_x$  planes.

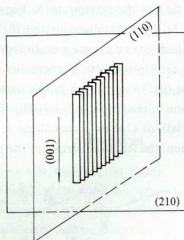


Fig.3 A model of spatial morphology of the plate-shaped bundle of *s'* phase laths

The group of the  $\{110\}_x$  have six crystallographic planes, among which each of the  $(110)$ ,  $(\bar{1}10)$ ,  $(101)$  and  $(\bar{1}01)$  planes have an angle of  $60^\circ$  with the foil plane  $(011)$ . There is a  $[001]$  orientation both in  $(110)$  and  $(\bar{1}10)$  planes, and a  $[010]$  orientation both in  $(101)$

and  $(\bar{1}01)$ . The projections of two orientations on the  $(01\bar{1})$  foil plane both are  $[100]$  orientation whose projection on  $(011)$  plane also is  $[100]$  orientation. Thus, it can be thought that the precipitate A in Fig.2 (a) is the projection of the plate-shaped bundle of  $s'$  phase laths lying on the  $(011)_x$  plane on the foil plane. Because it is perpendicular to the foil plane, the corresponding image of contrast is the narrowest, but still has a certain width, for the units of  $s'$  phase are lath-shaped and the bundles of the laths are not very thin. The precipitates B and C in Fig.2 (a) are considered as the projections on the foil plane for the plate-shaped bundles of  $s'$  phase laths precipitating on  $(110)_x$ ,  $(\bar{1}10)_x$ ,  $(101)_x$  and  $(\bar{1}01)_x$  planes. Because all of them have an angle of  $60(^\circ)$  with the foil plane, the width of the images are larger than that of the precipitate A. Fig.4 (a) is another bright field image of the  $(011)_x$  foil plane, which gives a clearer morphology of the  $s'$  phase. The precipitate F which lies on the foil plane  $(011)_x$  can be seen in this figure. The orientation of the stripes in F is  $[100]_x$ , showing that the lath of  $s'$  phase grows along  $\langle 100 \rangle_x$  orientation, the length of stripes in the precipi-

tate B or C is shorter than that in A and F, because  $[110]_x$  is parallel to  $(011)_x$  plane, while  $[010]_x$  and  $[0\bar{1}0]_x$  have an angle of  $45(^\circ)$  with the foil plane.

As for  $(110)_x$  foil plane, it has an angle of  $35(^\circ)$  with  $(110)$ ,  $(101)$  and  $(011)$  planes, and an angle of  $90(^\circ)$  with  $(\bar{1}10)$ ,  $(\bar{1}01)$  and  $(011)$  planes. There is a  $[001]$  orientation on  $(\bar{1}10)$  plane, a  $[010]$  orientation on  $(101)$  plane and a  $[100]$  on  $(011)$  plane. The projections of the three orientations on  $(011)_x$  foil plane are  $[11\bar{2}]$ ,  $[1\bar{2}1]$  and  $[2\bar{1}1]$  respectively, making an angle of  $60(^\circ)$  with each other, which correspond to the image in Fig.2 (c). Therefore, it is thought that the precipitates A, B and C are the projections on the  $(111)_x$  foil plane for the plate-shaped bundles of  $s'$  phase laths precipitated on  $(0\bar{1}1)_x$ ,  $(\bar{1}10)_x$  and  $(101)_x$  planes respectively.

The  $(211)_x$  foil plane makes an angle of  $30(^\circ)$  with the  $(110)$  and  $(101)$  planes. There is a  $[001]$  orientation on  $(110)$  plane and a  $[010]$  orientation on  $(101)$  plane. The angle of the two orientations with the  $(211)$  foil plane is  $24(^\circ)$ , and their projections on  $(211)$  plane are  $[215]$  and  $[2\bar{5}1]$  respectively. The angle of both  $(110)$  and  $(\bar{1}01)$  planes with the foil plane is

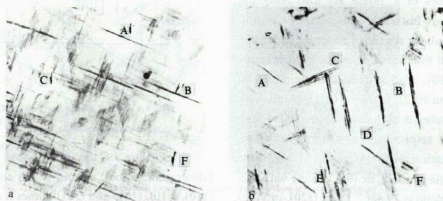


Fig.4 TEM micrographs showing the morphologies of  $s'$  phase in various foil planes in the sample aged at  $170^\circ\text{C}$  for 140 h

(a)— Bright field image of  $(011)_x$  foil plane; (b)— Bright field image of  $(211)_x$  foil plane

about  $73^\circ$ ). The (110) has an orientation of [001], and the (101) has a [010]. The angle between (011) and (211) is  $55^\circ$  and the [100] orientation on the (011) plane has an angle of  $54^\circ$  with the foil plane. The projection of the [100] on the foil plane is  $\bar{1}11$  orientation. The  $(0\bar{1}1)_x$  plane is perpendicular to the (211) foil plane. According to Fig.2 (e), it can be determined that the precipitate A lies on  $(011)_x$  plane, B on  $(\bar{1}10)_x$  plane and C on  $(\bar{1}01)_x$  plane. Such a result is just the same as that in Fig.2 (a) and (c). The width of the precipitates B and C is larger than that of A, because the angle of  $(\bar{1}10)$  or  $(\bar{1}01)$  planes with the (211) foil plane is less than that of the  $(0\bar{1}1)$  plane with the foil plane.

Another bright field image of the  $(211)_x$  foil plane is shown in Fig.4 (b), which gives the plate-shaped bundles of *s'* phase laths precipitated on all the six crystallographic plane in the group of  $\langle 110 \rangle_x$  zone planes. The precipitates A, B and C in Fig.4 (b) correspond to those in Fig.2. The orientation of the stripes is  $[2\bar{5}1]_x$  in the precipitate D,  $[21\bar{5}]_x$  in the precipitate E, and  $[111]$  in the precipitate F. It is not difficult to know that the precipitates D and E are the projections on the foil plane for the plate-shaped bundles lying on  $(101)_x$  and  $(110)_x$  planes. Because the angle of the two planes with the foil plane is only  $30^\circ$ , the image of the plates is wider, and their image contrast is weak. The precipitates D and E can also be seen in Fig.2(e), although the image is not clear. The precipitate F lies on  $(011)_x$  plane

which has an angle of about  $55^\circ$  with the  $(211)_x$  foil plane. This leads to the results that the width of precipitate F is larger than that of the precipitates B and C, but a bit smaller than that of E and D. Because the angle of  $[010]_x$  or  $[001]_x$  orientation with the  $(211)_x$  plane is  $24^\circ$ , and the angle between  $[100]_x$  and the foil plane is  $54^\circ$ , the length of the precipitates B, C, D and E is larger than that of the precipitates A and F.

## 5 CONCLUSIONS

(1) The units of *s'* phase in alloy of Al-1.94Li-2.36Cu-0.84Mg-0.07Zr are lath-shaped, and many *s'* phase units parallel each other get together to form a plate-shaped bundle of *s'* phase laths. The units of *s'* phase have habit planes of  $\{210\}_x$  and grow along  $\langle 100 \rangle_x$  orientation, but the plate-shaped bundles of *s'* phase laths lie on the  $\{110\}_x$  planes.

(2) When aged at  $170^\circ\text{C}$ , the appearance of the plate-shaped bundles of *s'* phase laths is more regular and the laths are thinner than that in the specimens aged at  $190^\circ\text{C}$ .

## REFERENCES

- 1 Silcock, J. M. J Inst Met, 1961, 89, 203.
- 2 Lorimer, C. W. In: Russel, K. C. *et al.* Eds. Precipitation Process in Solid, TMS-AIME, 1978, 87.
- 3 Sen, N. *et al.* J Inst Met, 1969, 97, 87.
- 4 Gregson, P. J. *et al.* Acta Metall, 1985, 33(3), 527.
- 5 Peel, C. J. *et al.* In: Starke, E. A. Jr. *et al.* Eds. Aluminium-Lithium Alloys II, TMS-AIME, 1984, 219.